

# Achievements of the Earth orientation parameters prediction comparison campaign

M. Kalarus · H. Schuh · W. Kosek · O. Akyilmaz · Ch. Bizouard · D. Gambis · R. Gross · B. Jovanović · S. Kumakshev · H. Kutterer · P. J. Mendes Cerveira · S. Pasynok · L. Zotov

Received: 4 November 2009 / Accepted: 18 May 2010 / Published online: 7 September 2010  
© Springer-Verlag 2010

**Abstract** Precise transformations between the international celestial and terrestrial reference frames are needed for many advanced geodetic and astronomical tasks including positioning and navigation on Earth and in space. To perform this transformation at the time of observation, that is for real-

time applications, accurate predictions of the Earth orientation parameters (EOP) are needed. The Earth orientation parameters prediction comparison campaign (EOP PCC) that started in October 2005 was organized for the purpose of assessing the accuracy of EOP predictions. This paper summarizes the results of the EOP PCC after nearly two and a half years of operational activity. The ultra short-term (predictions to 10 days into the future), short-term (30 days), and medium-term (500 days) EOP predictions submitted by the participants were evaluated by the same statistical technique based on the mean absolute prediction error using the IERS EOP 05 C04 series as a reference. A combined series of EOP predictions computed as a weighted mean of all submissions available at a given prediction epoch was also evaluated. The combined series is shown to perform very well, as do some of the individual series, especially those using atmospheric angular momentum forecasts. A main conclusion of the EOP PCC is that no single prediction technique performs the best for all EOP components and all prediction intervals.

---

M. Kalarus (✉) · W. Kosek  
Space Research Centre, Polish Academy of Sciences,  
ul. Bartycka 18A, 00-716 Warsaw, Poland  
e-mail: kalma@cbk.waw.pl

H. Schuh · P. J. M. Cerveira  
Institute of Geodesy and Geophysics, Vienna University  
of Technology, Gußhausstraße 27–29, 1040 Vienna, Austria

W. Kosek  
Environmental Engineering and Land Surveying,  
University of Agriculture in Kraków, Balicka 253A,  
30-198 Kraków, Poland

O. Akyilmaz  
Istanbul Technical University, Istanbul, Turkey

Ch. Bizouard · D. Gambis  
Paris Observatory, Paris, France

R. Gross  
Jet Propulsion Laboratory,  
California Institute of Technology, Pasadena, CA, USA

B. Jovanović  
Astronomical Observatory, Belgrade, Serbia

S. Kumakshev  
Institute for Problems in Mechanics,  
Russian Academy of Sciences, Moscow, Russia

H. Kutterer  
University of Hannover, Hannover, Germany

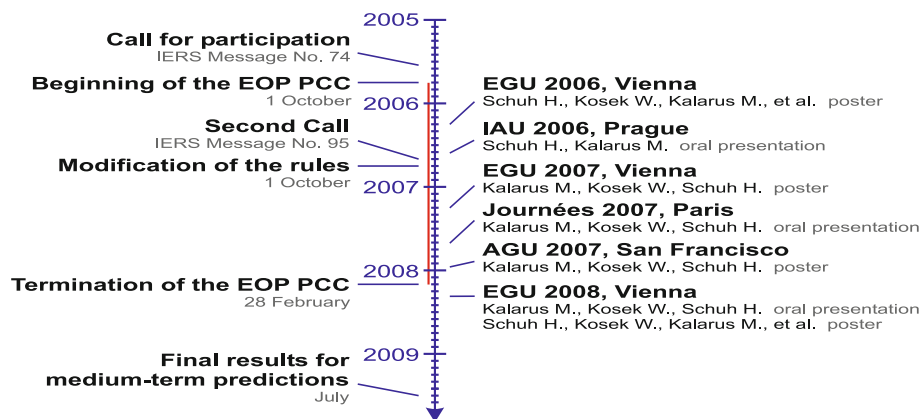
S. Pasynok · L. Zotov  
Moscow State University, Moscow, Russia

**Keywords** Earth orientation parameters · Predictions · Combined solution · Polar motion · UT1 · Universal time

## 1 Introduction

The advanced geodetic techniques enable determination of the Earth orientation parameters (EOP) with high accuracy up to 50–100  $\mu$ as in the case of  $x_p$ ,  $y_p$  pole coordinates and 5–10  $\mu$ s in the case of UT1–UTC data which corresponds to <3 mm on the Earth's surface. In practice, the EOP are computed using one or more independent space geodetic techniques (i.e. GPS, VLBI, DORIS, SLR, LLR) providing data with different availability, accuracy, and stability. The first rapid EOP data are computed from GPS observations

**Fig. 1** Calendar, events (*left side*), conferences (*right side*), *red line* operational part of the campaign



and then they are successively combined at the international Earth rotation and reference systems service (IERS) as soon as the next individual solutions are available. In that case their quality increases but at least one important problem still exists—due to the delay caused by computation procedures, the EOP determinations cannot be published in real time. Therefore, short-term EOP predictions are provided for many real-time applications including the tracking and navigating of interplanetary spacecrafts. EOP predictions can also be valuable for theoretical purposes to study the dynamics of various geophysical phenomena correlated with the EOP.

Regularly generated EOP predictions are provided by the IERS Rapid Service/Prediction Centre (McCarthy and Luzum 1991), the IERS EOP Product Centre, the Jet Propulsion Laboratory, and the EOP Service of the Institute for Astronomy and Astrophysics in Saint Petersburg, Russia. However, all prediction algorithms should be continually improved since the accuracy of the predictions even for a few days in the future are much worse than the accuracy of the observations (Kosek et al. 2008). These facts provided the background to the Earth orientation parameters prediction comparison campaign (EOP PCC), a project which aimed to investigate different strategies and techniques available to predicting EOP data. A further idea was to coordinate those working on EOP predictions to compare their results using well-defined rules, what is different from many previous (individual) studies.

The most important events related to the EOP PCC are given in Sect. 2. The list of participants and the rules of the campaign are presented in Sect. 3. An essential part of this work starts with a description of the input data used to compute the statistics. Issues linked with the IERS 97 C04 and 05 C04 time series are discussed in Sect. 4. Finally, the comprehensive results including the individual and combined solutions are discussed (Sect. 6). The results are supplemented by additional statistics (Sect. 5), which help to formulate the overall conclusions. Generally, the main objective of this

study is to make wide use of an unprecedented set of data that has never been collected before.

## 2 Milestones of the Earth orientation parameters prediction comparison campaign

The EOP PCC was prepared by the Vienna University of Technology with close cooperation of Polish Space Research Centre after discussing the idea within the IERS Directing Board. In July 2005 the “Call for participation” was officially announced as an IERS message no. 74 (IERS 2005). The operational stage of the EOP PCC started on October 1, 2005. In parallel, the official EOP PCC webpage (EOP PCC web page 2006) was created in order to provide up-to-date information, announcements, results, as well as all the related materials presented at international meetings and conferences (Fig. 1).

After 1 year (in October 2006) the rules of the campaign were changed slightly (IERS 2006) to fulfil the participants’ wishes. In the meantime new members joined the EOP PCC. In total, 13 participants (see the list of authors) from various countries and institutes contributed to this project. The operational phase was terminated at the end of February 2008 after collecting almost 6,500 submissions. There were 11 active participants at that time (Table 1) who provided EOP predictions computed by 20 prediction techniques denoted by ID numbers. Individual contributions (last column) are equal to the number of single files (submissions) accepted with respect to the formal correctness (name and data format) (Kalarus et al. 2007a).

## 3 Rules

The campaign supported predictions of all five EOP:  $x_p$ ,  $y_p$ , pole coordinates; UT1–UTC, universal time;  $\Delta$ , length of day; and  $dX$ ,  $dY$  (or  $d\psi$ ,  $d\epsilon$ ), precession–nutation

**Table 1** List of participants, prediction techniques, and total contribution as a number of sent files

| ID  | Participant           | Prediction technique  | Contribution |
|-----|-----------------------|---|--------------|
| 011 | S. Kumakshev          | Spectral analysis and least squares extrapolation (Akulenko et al. 2002a,b,c)   | 301          |
| 012 |                       | Spectral analysis and least squares extrapolation                               | 301          |
| 021 | O. Akyilmaz           | Wavelets and fuzzy inference systems  | 240          |
|     | H. Kutterer           |   |              |
| 031 | R. Gross              | Kalman filter (AAM forecast: NCEP) (Freedman et al. 1994; Gross et al. 1998)    | 885          |
| 051 | W. Kosek              | Combination of the least-squares extrapolation and autoregressive prediction    | 174          |
| 052 |                       | Wavelet decomposition and autocovariance prediction in polar coordinate system  | 174          |
| 053 |                       | Wavelet decomposition and autocovariance prediction                             | 370          |
| 061 | M. Kalarus            | Least squares extrapolation of the harmonic model and autoregressive prediction | 449          |
| 071 | EOP Product Centre    | Least squares and autoregressive filtering                                      | 611          |
| 072 | D. Gambis             | Adaptive transformation from AAM to LODR (AAM forecast: JMA)                    | 78           |
| 073 |                       | Adaptive transformation from AAM to LODR (AAM forecast: NCEP)                   | 76           |
| 074 |                       | Adaptive transformation from AAM to LODR (AAM forecast: UKMO)                   | 76           |
| 075 |                       | Adaptive transformation from AAM to LODR (AAM forecast: JMA + NCEP + UKMO)      | 74           |
| 091 | L. Zotov              | Autoregressive prediction   | 495          |
| 092 |                       | Least squares collocation   | 495          |
| 093 |                       | Neural networks   | 495          |
| 101 | S. Pasyok             | Autoregressive prediction with consecutive shift                                | 282          |
| 111 | P. J. Mendes Cerveira | Heuristic analysis and least squares fitting/extrapolation                      | 204          |
| 112 |                       | Least squares fitting/extrapolation for amplitudes of Legendre polynomials      | 274          |
| 121 | B. Jovanović          | HE (harmonic and exponential) method of approximation (Jovanović 1987, 1989)    | 122          |

residuals. The predictions were divided into three categories: ultra short-term for <10 days, short-term for <30 days, and medium-term for <500 days. The assumption is that high and low frequency variations of the EOP can be driven by different geophysical phenomena and consequently different prediction strategies should be applied. From the participants' point of view, this provided the opportunity to choose particular prediction techniques and algorithms which were only appropriate for certain EOP data and for certain prediction length. However, for practical reasons there is no need to collect ultra short-term and short-term predictions of  $dX$  and  $dY$  or  $d\psi$  and  $d\varepsilon$ , because the current IAU2000/IAU2006 precession–nutration model (McCarthy and Petit 2004) fits very well to the observations (the prediction of  $d\psi$  and  $d\varepsilon$  was based on the KSV\_1996\_3 model (McCarthy 1996)). In that case only medium-term predictions may be interesting, as the Free Core Nutation with a period around 432 days has shown strong variability of amplitude and frequency/phase (Kosek et al. 2006) in the last few decades (Kalarus et al. 2006). According to the rules, each participant could apply more than one prediction technique to the same EOP data. In addition, no recommendations for the predictions were given allowing participants the freedom in choosing their own best prediction method and input data. It was stated that the results would be compared with the IERS C04 series. Of course, all predictions had to be

submitted using proper name (filename) and format (EOP-PPCC web page 2006). Finally, as the most important rule of the campaign, all the predictions had to be submitted every week on Thursday at noon (UTC) before any new EOP observations were available (e.g. the predictions starting from January 4, 2008 had to be submitted on January 3, 2008).

## 4 Data sets

### 4.1 IERS EOP 97 C04 versus EOP 05 C04

As mentioned before, the official EOP PCC statistics were originally referred to the IERS EOP 97 C04 series. However, in mid-2007, the new IERS EOP 05 C04 series (consistent with the ITRF 2005) was released and the IERS Earth Orientation Centre discontinued the C04 series on October 11, 2007 (Bizouard and Gambis 2005). This caused some problems since there were no reference data for the predictions based on 97 C04 series that went beyond October 11, 2007.

In order to find a simple and common way to compare all predictions, the differences between 97 C04 and 05 C04 have been studied in terms of each EOP and each prediction category. In the case of  $x_p$ ,  $y_p$ , UT1–UTC, and  $\Delta$  the differences are rather small and residual trends are not visible. Therefore

only the IERS EOP 05 C04 were used as a reference for those EOP data within all categories. However, predictions of  $x_p$  and  $y_p$  sent before July 2007 were initially corrected by the offset values equal to  $-0.1$  and  $0.3$  mas, respectively (IERS 2007). This still rises a question about the accuracy of the statistics for ultra short-term predictions which are the most sensitive to any disagreement between the reference series. In fact, participants who were using C04 as their input data did not switch from the *old* to *new* series at the same epoch. To avoid possible doubts, the maximum possible changes that could have affected the final statistics by using this approach were computed (see Sect. 6 for more details).

Unfortunately, more difficulties occurred when comparing the *old* (97 C04) and *new* (05 C04) precession–nutration residuals (Bizouard and Gambis 2005). Significant differences make it impossible to refer the 97 C04 based predictions ( $dX$ ,  $dY$ ,  $d\psi$ ,  $d\epsilon$ ) to the 05 C04 time series and vice versa. Thus, a reasonable way to compute statistics was to match those predictions with the correct reference data. After the division of the predictions into two sets (based on 97 C04 and 05 C04), it turns out that there were not enough predictions based on 97 C04 because only one participant could be taken into account. In contrast, there were slightly more 05 C04 based predictions (submitted by participants who joined the campaign later) but still not enough to perform reasonable comparisons of the prediction algorithms. For this reason, the present work does not include results for the precession–nutration residuals. On the other hand such predictions are less important for practical reasons. This could also explain their low popularity within the campaign. Additionally, the stochastic part of the precession–nutration residuals has much smaller variance than the variance of the stochastic part of the  $x_p$  and  $y_p$  pole coordinates.

### 4.2 Participants’ submissions

Considering some limitations of the objectives, the entire set of accepted predictions (those listed in Table 1) cannot be used for the computation of the statistics. First, the number of predictions decreased according to the availability of the reference data, as was already described. Second, some highly inaccurate predictions strongly disturbed the preliminary results of the mean prediction error computations and had to be disregarded. It is believed that those bad submissions were caused mainly by human mistake rather than by the prediction algorithm. Thus, they were removed from further analyses by using the threshold computed from the median absolute prediction error MDAE defined here for the  $i$ th day in the future

$$MDAE_i = \text{median} (|\epsilon_{i,1}|, |\epsilon_{i,2}|, \dots, |\epsilon_{i,j}|, |\epsilon_{i,n_a}|), \quad (1)$$

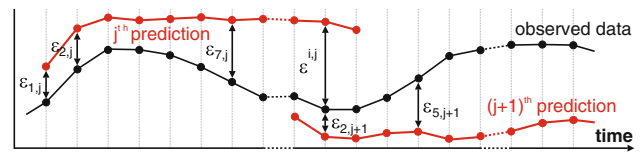


Fig. 2 Observed data and predictions

where  $\epsilon_{i,j}$  denotes the differences between the observed EOP data and their  $i$ th point of  $j$ th prediction (see Fig. 2).

$$\epsilon_{i,j} = x_i^{\text{obs}} - x_{i,j}^{\text{pred}} \quad (2)$$

The MDAE was then computed for each EOP data set and each category considering all ( $n_a$ ) relevant predictions. In addition, the relative quality  $\beta_j$  with respect to MDAE was evaluated for each single prediction

$$\beta_j = \sum_{i=1}^I (\alpha \cdot MDAE_i - |\epsilon_{i,j}|), \quad (3)$$

where  $I$  denotes the length of prediction. Then, if  $\beta_j < 0$  the prediction was not included in the further studies, while the  $\alpha$  coefficient was deduced empirically ( $\alpha = 5$ ) to preserve a representative set of data.

Finally, the set of formally accepted predictions was reduced by 2% due to highly inaccurate predictions (see Table 2 for more details).

This analysis and the rest of data processing were performed with the same rules using original software written in *Matlab v7.4*

## 5 Statistics

The key problem of the EOP PCC was to find an objective way to compare predictions with respect to the same observed data. Among the various statistical estimates the mean absolute error (MAE) was selected as the primary statistical measure. The MAE is defined for the  $i$ th day in the future by the following

$$MAE_i = \frac{1}{n_p} \sum_{j=1}^{n_p} |\epsilon_{i,j}|, \quad i = 1, 2, \dots, I, \quad (4)$$

where  $n_p$  is the number of predictions related to the same ID and the same EOP data. This basic estimate still must be used together with some additional information. In fact, a comprehensive analysis has to deal with the prediction data files being non-contemporaneous (see Fig. 3) as the different participants submitted a different number of predictions. Thus, supplementary statistical parameters are introduced and discussed in the following sections.

**Table 2** Number of used and rejected predictions; ultra short-term (blue), short-term (green), medium-term (red)

| ID       | 011                    | 012                   | 021                   | 031                   | 051                  | 052                  | 053          | 061                   | 071                   | 072  | 073  | 074  | 075  | 091                   | 092                   | 093                   | 101                     | 111                  | 112                  | 121                  |
|----------|------------------------|-----------------------|-----------------------|-----------------------|----------------------|----------------------|--------------|-----------------------|-----------------------|------|------|------|------|-----------------------|-----------------------|-----------------------|-------------------------|----------------------|----------------------|----------------------|
| $x_p$    | 124/3<br>87/0<br>87/0  | 127/0<br>87/0<br>87/0 | 80/0<br>40/0<br>13/27 | 125/0<br>85/0<br>85/0 | 87/0<br>87/0<br>87/0 | 87/0<br>87/0<br>87/0 |              | 127/0<br>87/0<br>87/0 | 108/0<br>69/0<br>47/0 |      |      |      |      | 105/0<br>60/0<br>60/0 | 105/0<br>60/0<br>60/0 | 105/0<br>60/0<br>60/0 | 43/0<br>43/0<br>43/0    | 68/0<br>68/0<br>68/0 |                      |                      |
| $y_p$    | 116/11<br>82/5<br>87/0 | 127/0<br>87/0<br>87/0 | 79/1<br>38/2<br>7/33  | 124/1<br>85/0<br>85/0 | 87/0<br>87/0<br>87/0 | 87/0<br>87/0<br>87/0 |              | 127/0<br>87/0<br>87/0 | 108/0<br>68/1<br>47/0 |      |      |      |      | 105/0<br>60/0<br>60/0 | 105/0<br>60/0<br>60/0 | 104/1<br>60/0<br>60/0 | 10/31<br>13/28<br>13/28 | 63/5<br>60/8<br>68/0 |                      |                      |
| UT1-UTC  |                        |                       |                       | 123/2<br>85/0<br>85/0 |                      |                      | 74/0<br>73/1 |                       | 104/4<br>68/1<br>46/1 | 56/1 | 56/0 | 55/1 | 55/0 | 105/0<br>60/0<br>60/0 | 105/0<br>60/0<br>60/0 | 104/1<br>60/0<br>60/0 | 10/31<br>13/28<br>13/28 |                      | 1/0<br>1/0<br>1/0    | 45/2<br>42/1<br>31/1 |
| $\Delta$ |                        |                       | 80/0                  | 125/0<br>85/0<br>85/0 |                      |                      | 74/0<br>73/1 | 74/0<br>74/0          | 54/0<br>55/0<br>41/0  | 20/1 | 19/1 | 19/1 | 18/1 | 104/1<br>60/0<br>60/0 | 99/6<br>59/1<br>59/1  | 103/2<br>59/1<br>59/1 | 12/0<br>12/0<br>12/0    |                      | 67/1<br>68/0<br>68/0 |                      |

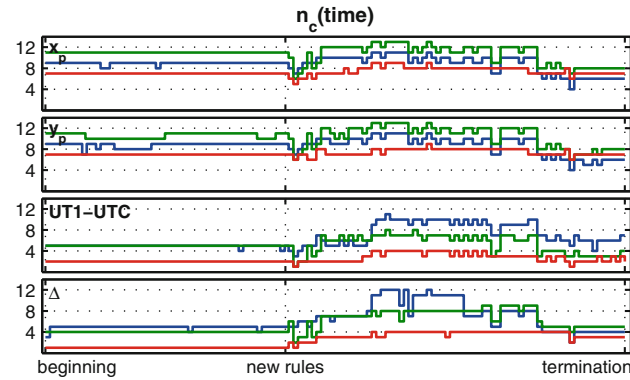


**Fig. 3** Number  $n_c$  of available predictions with respect to prediction epoch; ultra short-term (blue), short-term (green), medium-term (red)

5.1 Combined solution

As already mentioned a data set containing a few thousands predictions was analyzed here. However, the most interesting fact was that in some cases there were more than ten individual predictions available at the same epoch (Fig. 3). This led to the question of whether it was possible to combine those solutions and what advantages could be expected from such a combination.

5.1.1 Distribution of the prediction residuals

In the first step, a distribution of the prediction residuals  $\epsilon_{i,j}$  was computed to check the possibility of applying the rule of Gaussian error propagation. Figure 4 shows that the prediction residuals for the first and fifth day in the future are reasonably Gaussian. Therefore, combined solutions might be superior due to the averaging process reducing the effect of the random errors of each individual prediction series (Luzum et al. 2007).

As a second step, more detailed analysis of the prediction residuals for the first and fifth day in the future of the  $x_p$  pole coordinate data were performed. Table 3 presents four statistical estimators describing Gaussian-like time series: mean value ( $\hat{\mu}$ ), standard deviation ( $\hat{\sigma}$ ), skewness ( $\hat{s}$ ), and excess kurtosis ( $\hat{k}$ ), where the last two estimators give an idea about

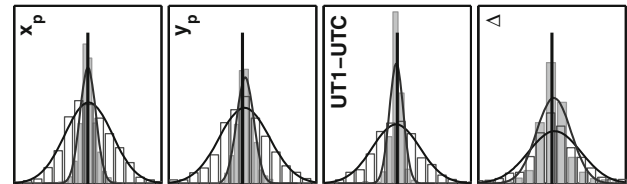


**Fig. 4** Distributions of the first day (grey) and fifth day (white) prediction residuals compared with the best-fitted normal distributions, respectively

**Table 3** Mean value ( $\hat{\mu}$ ), standard deviation ( $\hat{\sigma}$ ), skewness ( $\hat{s}$ ), and kurtosis ( $\hat{k}$ ) of the prediction residuals for the first day (dark grey) and fifth day (light grey) in the future of  $x_p$  pole coordinate data

| ID  | mean [mas] |      | $\sigma$ [mas] | skewness |      | kurtosis |      |
|-----|------------|------|----------------|----------|------|----------|------|
|     | -1.20      | 1.20 | 5.00           | -0.70    | 0.70 | -2.00    | 2.00 |
| 011 |            |      |                |          |      |          |      |
| 012 |            |      |                |          |      |          |      |
| 021 |            |      |                |          |      |          |      |
| 031 |            |      |                |          |      |          |      |
| 051 |            |      |                |          |      |          |      |
| 052 |            |      |                |          |      |          |      |
| 053 |            |      |                |          |      |          |      |
| 061 |            |      |                |          |      |          |      |
| 071 |            |      |                |          |      |          |      |
| 072 |            |      |                |          |      |          |      |
| 073 |            |      |                |          |      |          |      |
| 074 |            |      |                |          |      |          |      |
| 075 |            |      |                |          |      |          |      |
| 091 |            |      |                |          |      |          |      |
| 092 |            |      |                |          |      |          |      |
| 093 |            |      |                |          |      |          |      |
| 101 |            |      |                |          |      |          |      |
| 111 |            |      |                |          |      |          |      |
| 112 |            |      |                |          |      |          |      |
| 121 |            |      |                |          |      |          |      |
| all |            |      |                |          |      |          |      |

asymmetry and flatness relative to the normal distribution, respectively. The appropriate equations are written as follows (Tabachnick and Fidell 1996):

$$\hat{\mu}_i = \frac{1}{n_p} \sum_{j=1}^{n_p} \epsilon_{i,j}, \quad \hat{\sigma}_{\hat{\mu}_i} = \frac{\hat{\sigma}_i}{\sqrt{n_p}}, \quad (5)$$

$$\hat{\sigma}_i = \sqrt{\frac{\sum_{j=1}^{n_p} (\epsilon_{i,j} - \hat{\mu}_i)^2}{n_p - 1}}, \quad \hat{\sigma}_{\hat{\sigma}_i} = \frac{\hat{\sigma}_i}{\sqrt{2n_p}}, \quad (6)$$

$$\hat{s}_i = \sum_{j=1}^{n_p} \frac{(\varepsilon_{i,j} - \hat{\mu}_i)^3}{(n_p - 1)\hat{\sigma}_i^3}, \quad \hat{\sigma}_{\hat{s}_i} = \sqrt{\frac{6}{n_p}}, \quad (7)$$

$$\hat{k}_i = \sum_{j=1}^{n_p} \frac{(\varepsilon_{i,j} - \hat{\mu}_i)^4}{(n_p - 1)\hat{\sigma}_i^4} - 3, \quad \hat{\sigma}_{\hat{k}_i} = \sqrt{\frac{24}{n_p}}. \quad (8)$$

As can be seen in Table 3, the mean value  $\hat{\mu}_i$  is subjected to a relatively big error caused by the small number of prediction files. In that case there is no clear evidence whether the individual algorithms give biased (in case the mean value of prediction residuals differs from zero) solutions or not. The second parameter  $\hat{\sigma}$ , is related to the quality of the prediction and plays an important role in this study. Interesting behavior can also be detected by the skewness and the kurtosis parameters. Many of the individual predictions have a positive value of  $\hat{s}$  (the right tail is stronger than the left one) and negative value of  $\hat{k}$  (distribution is flat relative to a normal one). However, predictions for the first day in the future have a positive value of  $\hat{k}$  (distribution is peaked relative to a normal one). The problem is that those values are not statistically significant because their errors usually are greater than these values (Table 3). To reduce these errors, the time span of the EOP PCC should have been longer than it was.

### 5.1.2 Correlations of the predictions

The main idea of the combined solution  $S_C$  is simply based on the weighted  $w$  mean of individual submissions  $S_I$  available at a given prediction epoch. It can be described by the equation

$$S_C = \frac{1}{n_c} \sum_{k=1}^{n_c} w_k S_{I_k} \quad (9)$$

with the resultant standard deviation

$$\hat{\sigma}_{S_C} = \frac{1}{n_c} \sqrt{\sum_{j=1}^{n_c} \sum_{k=1}^{n_c} \hat{c}_{j,k} w_j \hat{\sigma}_j w_k \hat{\sigma}_k}, \quad (10)$$

where the  $\hat{c}_{j,k}$  is the cross-correlation coefficient,  $w_j$  is the weight, and  $n_c$  is the number of available predictions for a given prediction epoch. In other words, the combined solution gets better (has smaller  $\hat{\sigma}_{S_C}$ ) if the individual predictions or the prediction residuals (which is the same in this case) are negatively correlated. In fact, one might expect that the outputs of similar prediction techniques would be correlated with each other. This is confirmed in Fig. 5 which shows the correlation coefficients  $\hat{c}$  between prediction residuals for the 5-day prediction (only lower or upper triangular part).

Crosses inside these matrices mean that the values of  $\hat{c}$  would not be meaningful due to the insufficient (<30) number of common data points. The most significant correlation coefficients are clear in the case of the prediction algo-

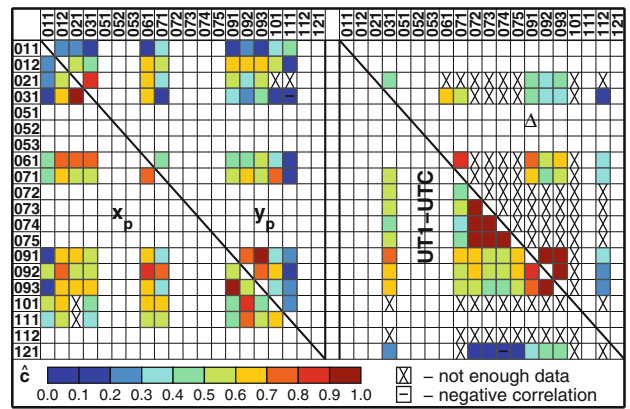


Fig. 5 Correlation of fifth day prediction residuals (ultra short-term predictions) of  $x_p$ ,  $y_p$ , UT1–UTC, and  $\Delta$

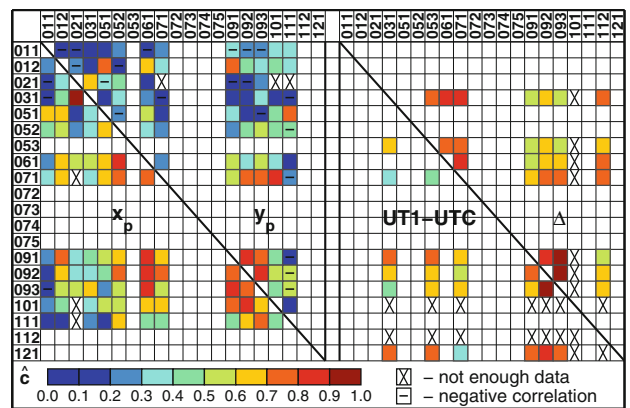
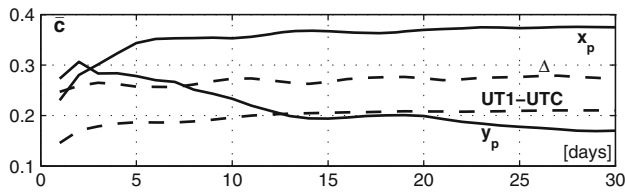


Fig. 6 Correlation of 30th day prediction residuals (short-term predictions) of  $x_p$ ,  $y_p$ , UT1–UTC, and  $\Delta$

gorithms marked by ID 072, 073, 074, and 075—predictions of UT1–UTC (Fig. 5). It confirms that these are the same algorithms and the only difference occurs in application of the atmospheric angular momentum (AAM) inputs (see Table 1). On the other hand, there is also a high correlation between the outputs from algorithms 091, 092, and 093 for the predictions of UT1–UTC and  $\Delta$  (Fig. 5). This is surprising because those techniques were declared as different (Table 1). One can also see the dominance of positive correlations coefficients with a few exceptions only. This means that most of the ultra short-term predictions tend to go to the same direction (positive or negative) with respect to the observed EOP data and that there are irregular variations in the data which cannot be predicted with the current set of algorithms.

Analogous correlation coefficient matrices were computed for 30-day predictions (Fig. 6). These, like the previous analysis, are positively correlated, but only in the case of  $x_p$ , UT1–UTC, and  $\Delta$ . The correlation coefficients for  $y_p$  are smaller (or even negative), which affects the combined solution. More general properties are depicted in Fig. 7 showing



**Fig. 7** Mean correlation of the prediction residuals (short-term predictions) of  $x_p$ ,  $y_p$ , UT1–UTC, and  $\Delta$

the mean cross-correlation coefficients as a function of the prediction length.

It gives an idea about the similarity of the prediction techniques proposed by different participants or groups. Here, the most remarkable behavior of the statistic occurs for pole coordinates since the mean cross-correlation coefficients are significantly smaller for  $y_p$  than for  $x_p$ . This means that short-term and medium-term oscillations (and also linear trend) in  $y_p$  are more difficult to predict. As a conclusion one may also notice that the strong positive correlation coefficients decrease the accuracy of the combined predictions (Eq. 10).

5.1.3 Weighting

According to Eq. (10), the quality of the combined solution depends on the weights  $w$  and the correlation coefficients  $\hat{c}$  between the individual predictions. The value of  $\hat{c}$  is already fixed, therefore minimization of  $\sigma_{CS}$  was performed with respect to the weights which lead to the relation

$$w_i \sim \frac{1}{\hat{\sigma}^2}, \quad \sum w_i = 1. \tag{11}$$

where

$$\hat{\sigma} = \frac{1}{n_I} \sum_{i=1}^{n_I} \hat{\sigma}_i, \tag{12}$$

and  $n_I$  depends on the prediction category ( $n_I = 10, 30,$  or  $500$ ). However, the practical tests showed that the terms associated with the bias (Eq. 5) and number of predictions  $n_p$  (Eq. 6) have to be considered as well. The variance (Eq. 11) was then replaced by the root mean square (rms)

$$\hat{m}s^2 = \hat{\mu}^2 + \hat{\sigma}_{\hat{\mu}}^2 \tag{13}$$

and the final weights (see Table 4)

$$w \sim \left( \frac{2n_p}{\hat{m}s^2} \right)^2, \quad \sum w = 1. \tag{14}$$

were adjusted by means of empirical evaluation. In this case the higher weights are related to more accurate (smaller standard deviation) and reliable (high value of  $n_p$ ) predictions.

**Table 4** Contributions [weights(%)] to the combined solution; ultra short-term (blue), short-term (green), medium-term (red)

|          | %  | 011 | 012 | 021 | 031 | 051 | 052 | 053 | 061 | 071 | 072 | 073 | 074 | 075 | 091 | 092 | 093 | 101 | 111 | 112 | 121 |
|----------|----|-----|-----|-----|-----|-----|-----|-----|-----|-----|-----|-----|-----|-----|-----|-----|-----|-----|-----|-----|-----|
| $x_p$    | 80 | 10  | 10  | 10  | 10  | 10  | 10  | 10  | 10  | 10  | 10  | 10  | 10  | 10  | 10  | 10  | 10  | 10  | 10  | 10  | 10  |
| $y_p$    | 80 | 10  | 10  | 10  | 10  | 10  | 10  | 10  | 10  | 10  | 10  | 10  | 10  | 10  | 10  | 10  | 10  | 10  | 10  | 10  | 10  |
| UT1-UTC  | 60 | 10  | 10  | 10  | 10  | 10  | 10  | 10  | 10  | 10  | 10  | 10  | 10  | 10  | 10  | 10  | 10  | 10  | 10  | 10  | 10  |
| $\Delta$ | 80 | 10  | 10  | 10  | 10  | 10  | 10  | 10  | 10  | 10  | 10  | 10  | 10  | 10  | 10  | 10  | 10  | 10  | 10  | 10  | 10  |

6 Results

The most remarkable statistics of the campaign are presented in Fig. 8 which shows the MAE (Eq. 4) of the predictions of all EOP ( $x_p$ ,  $y_p$ , UT1–UTC, and  $\Delta$ ) and categories. Additional information can also be obtained from the error bars

$$\hat{\sigma}_{MAE_i} = \frac{\hat{\sigma}_i}{\sqrt{nc}}, \quad c = \frac{\pi}{\pi - 2}, \quad \hat{\mu}_i \simeq 0 \tag{15}$$

computed for the last prediction day of a given category (10th, 30th, or 500th) and value of  $n$  that is proportional to the number of predictions  $n_p$ . Each participant or group has his own color but for those who had provided more than one prediction technique, dotted and dashed lines are used. However, for the sake of clarity, the results with relatively small  $n_p$  (<15% of the maximum possible value) were not shown in the figure. The black circled lines in Fig. 8 denote the combined solutions which were computed only when at least three individual submissions were available at a given prediction epoch.

For most practical applications ultra short-term predictions are needed. Their minimum one day prediction errors are at the level of 0.5 mas for  $x_p$ , 0.35 mas for  $y_p$ , 0.08 ms for UT1–UTC, and 0.05 ms/day for  $\Delta$ , which is still large in comparison to the current formal errors  $\sigma_{EOP}$  (shown on the plots) associated with the EOP estimates (Bizouard and Gambis 2005). These results are supplemented by adding parameter  $\delta$  which is the maximum uncertainty of the results due to differences between 97 C04 and 05 C04. The values of  $\delta$  and  $n$  have to be considered before making any firm conclusions. In each category the combined solution provides the best prediction (Kalarus et al. 2007b, 2008) or is very close to the best individual solution: 061 in case of pole coordinates data and 031 in case of UT1 and  $\Delta$  data.

Some interesting results can be seen in the short-term prediction category of the  $x_p$  and  $y_p$  pole coordinates data. Here, the combined solution is clearly the best, especially in

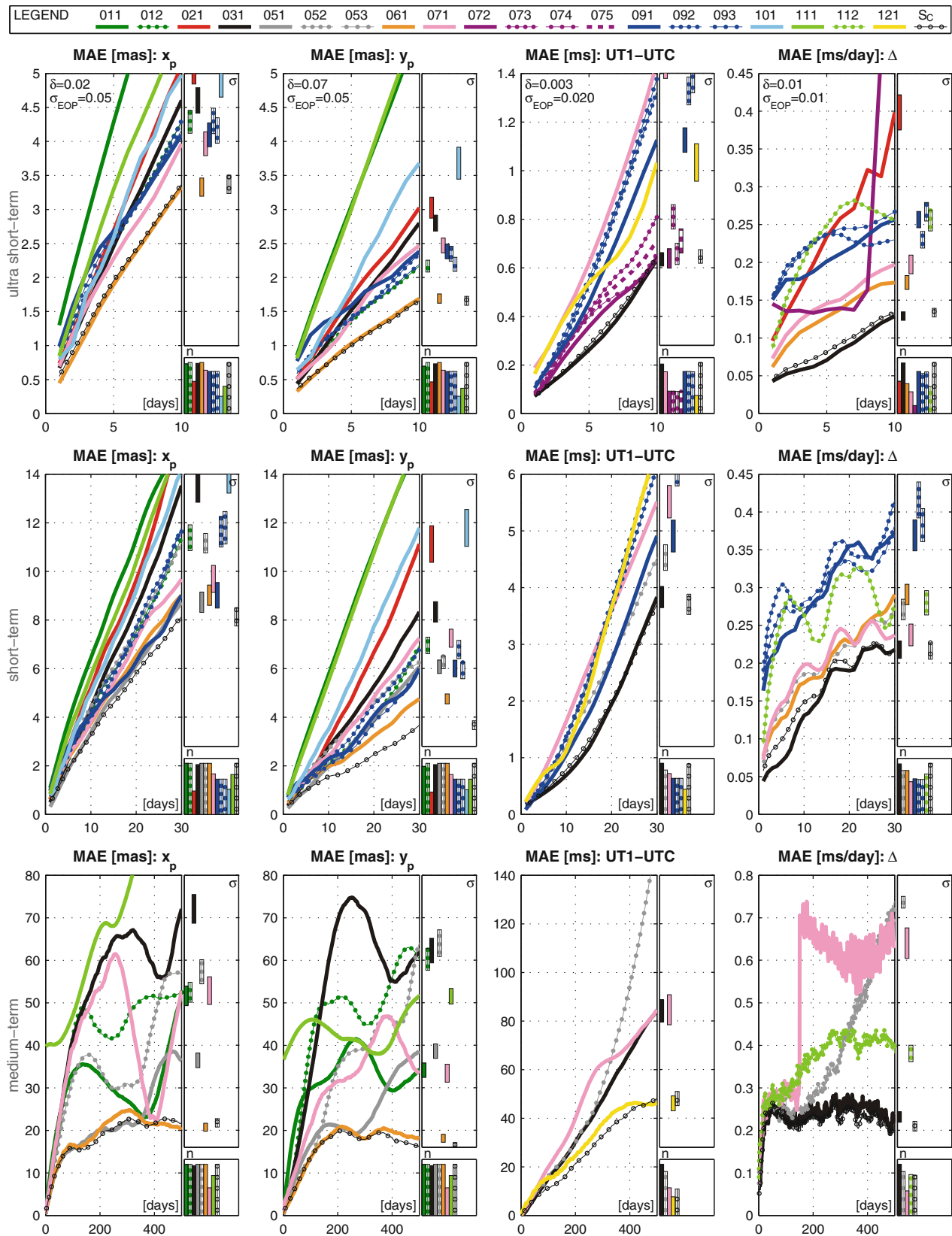


**Fig. 8** Mean absolute prediction errors (MAE) of  $x_p$ ,  $y_p$ ,  $\Delta$  and UT1-UTC data computed for all categories,  $\delta$  maximum uncertainty due to differences between 97 C04 and 05 C04,  $\sigma_{EOP}$  precision of the EOP

solution,  $\sigma$  standard deviation of the solution computed for the last prediction day,  $n$  indicator of the relative number of predictions used to compute MAE



**Table 5** The most accurate prediction techniques participating in the EOP PCC for  $x_p$ ,  $y_p$  pole coordinates

| Prediction technique                                   |
|--|
| LS extrapolation of the harmonic model + AR prediction |
| Spectral analysis + LS extrapolation                   |
| Neural networks  |

**Table 6** The most accurate prediction techniques participating in the EOP PCC for UT1–UTC and  $\Delta$ 

| Prediction technique                              |
|---|
| Kalman filter (AAM forecast: NCEP)                |
| Wavelet decomposition + autocovariance prediction |
| Adaptive transformation from AAM to LODR          |

the case of  $y_p$ , as expected after looking at its small cross-correlations (Fig. 6) and mean cross-correlations (Fig. 7). This relatively high accuracy of the combined solution is also due to the large number of individual predictions available at a given prediction epoch (Fig. 3). The results of the medium-term category do not reveal any particular properties and, like the ultra short-term predictions, the combined solution follows the best individual solution.

Accuracy of the combined solution mostly corresponds to the cross-correlations between the individual solutions and also to the number of submissions available at each prediction epoch. Low cross-correlation between individual predictions increase the accuracy of the combined solution. However, different predictions can be almost the same. Their mean cross-correlations are positive at the level of 0.2–0.4 (for the various EOP) with the exception of  $y_p$  where it gets smaller for longer predictions. It is also important to note that this solution is evaluated a posteriori after investigating the statistical parameters of the individual submissions.

In some cases, it is difficult to say precisely which mean prediction errors are smaller due to the size of the error bars. Finally, the value of  $n$  is related to the relative number of predictions used. This allows the identification of participants who joined the campaign later or had stopped sending their submissions before the end of the campaign.

The results showed in Fig. 8 can be summarized in Tables 5 and 6 presenting the best individual prediction techniques for  $x_p$ ,  $y_p$  and UT1–UTC,  $\Delta$ , where the numerical order indicates decreasing prediction performance. It can be noticed that different strategies should be applied to predict equatorial and axial component of the Earth rotation vector. The situation is probably determined by the current state of the art in EOP predicting and also by the availability and accuracy of additional inputs [i.e. AAM, oceanic angular momentum (OAM), hydrological angular momentum (HAM) data and forecast] that can be assimilated by the algorithms. Further

analysis shows that in some cases, the best prediction method for short-term is not the best for medium-term for the same component (Fig. 8). This occurs due to different origin of oscillations in EOP—the first are dominated by wide-band short period variations (Kosek 2010a,b), and the second by irregular variations of the most energetic oscillations, e.g. Chandler and annual (Kosek et al. 2006).

The reader should also note that the presented results are valid for the limited period of the EOP PCC and may differ from statistics computed for other periods. Consequently, the prediction accuracies claimed by the EO Centre and the Rapid Service and Prediction Centre (IERS Annual Report 2007) cannot be directly compared with the results of the campaign, but it appears that the campaign has found a considerably better UT1 prediction method.

## 7 Summary

The EOP PCC was a great innovative opportunity to bring scientists together from various countries and institutes to work in competitive mode on improvement of the EOP predictions. Thanks to the participants, their effort, knowledge, and experience, an unprecedented set of predictions was collected during the operational part (29 months) of the EOP PCC. It demonstrated several valuable conclusions that were not so obvious before the campaign.

The main results show that the EOP PCC was useful as a first attempt to evaluate the various existing prediction techniques under the same rules and conditions. The advantages of using a combined solution are clearly indicated as the combined series very often performs better than all individual predictions techniques and is quite naturally more reliable and robust with respect to mistakes or human errors. Accuracy of the predictions also benefits from using atmospheric forecasts data as an input. However, some statistical parameters have been estimated with relatively high error that is due to the insufficient number of submissions. In this context the campaign was too short to come to firm conclusions. It is especially proven by Figs. 3 and 8 where the large error bars do not allow a comprehensive comparison of all the results.

Nevertheless, the EOP PCC provided valuable insight into the difficult task of predicting the Earth rotation vector. For instance, the best prediction technique is different for different categories (parameter to be predicted and prediction length), i.e. there is not one particular prediction technique superior to the others for all EOP and all prediction intervals.

The analysis leads to the conclusion that any continuation of the campaign or of a similar study is recommended to improve the results by decreasing their standard deviation and to reveal some possible additional statistical parameters. Different scenarios can be considered in order to increase

the number of collected submissions. A valuable test of prediction algorithms may consider usage of the historical EOP observations that also include El-Niño events.

As the prediction accuracy benefits from AAM forecast data, more attention should be put on the analysis and prediction of the AAM, OAM, and HAM. This can then be valuable for many theoretical and practical purposes, as it was mentioned at the beginning of this paper.

As a consequence of the many valuable conclusions that could be drawn from the EOP PCC but also with respect to many remaining open questions a Working Group on Prediction (WGP) was established within the IERS in 2006 and the topic of prediction was also thoroughly discussed on an IERS Workshop held in Warsaw in October 2009.

**Acknowledgments** Maciej Kalarus is grateful to the Advisory Board of the “Descartes-nutation project” for the financial support. The work of RG described in this paper was performed at the Jet Propulsion Laboratory, California Institute of Technology, under contract with the National Aeronautics and Space Administration. We are grateful to Editor-in-Chief for his comments on the manuscript. We also thank Jeff Freymeuller, Jim Ray, and one anonymous reviewer for helpful remarks which led to an improvement of the paper.

## References

- Akulenko LD, Kumakshev SA, Markov YuG (2002) Motion of the Earth’s pole. *Dokl Phys* 47:78–84
- Akulenko LD, Kumakshev SA, Markov YuG, Rykhlova LV (2002) A model for the polar motion of the deformable Earth adequate for astrometric data. *Astron Rep* 46:74–82
- Akulenko LD, Kumakshev SA, Markov YuG, Rykhlova LV (2002) Forecasting the polar motions of the deformable Earth. *Astron Rep* 46:858–866
- Bizouard Ch, Gambis D (2005) The combined solution C04 for Earth orientation parameters consistent with international terrestrial reference frame 2005. Observatoire de Paris. [http://hpiers.obspm.fr/eoppc/eop/eopc04\\_05/C04\\_05\\_guide.pdf](http://hpiers.obspm.fr/eoppc/eop/eopc04_05/C04_05_guide.pdf)
- EOPPC (2006) Earth orientation parameters prediction comparison campaign. [http://www.cbk.waw.pl/EOP\\_PCC](http://www.cbk.waw.pl/EOP_PCC)
- Freedman AP, Steppe JA, Dickey JO, Eubanks TM, Sung LY (1994) The short-term prediction of universal time and length of day using atmospheric angular momentum. *J Geophys Res* 99:6981–6996
- Gross RS, Eubanks TM, Steppe JA, Freedman AP, Dickey JO, Runge TF (1998) A Kalman filter-based approach to combining independent Earth orientation series. *J Geodesy* 72:215–235
- IERS (2005) IERS Central Bureau. IERS message no. 74. <http://www.iers.org>
- IERS (2006) IERS Central Bureau. IERS message no. 95. <http://www.iers.org>
- IERS (2007) IERS Central Bureau. IERS message no. 113. <http://www.iers.org>
- Jovanović B (1987) An approximation of tabulated function. *Publ. Inst. Math. Belgrad* 41(55):143–148
- Jovanović B (1989) An analytical representation of ephemeris data. *Celest Mech* 45:317–320
- Kalarus M, Kosek W, Schuh H (2007a) Current results of the Earth orientation parameters prediction comparison campaign. In: Capitaine N (ed) *Proceedings of the journées 2007, systèmes de référence spatio-temporels “The celestial reference frame for the future”*. Observatoire de Paris Systemes de Référence Temps-Espace UMR8630/CNRS, Paris, France, pp 159–162
- Kalarus M, Kosek W, Schuh H (2007b) Current results of the Earth orientation parameters prediction comparison campaign. In: AGU fall meeting 2007, San Francisco, California, Earth’s reference system and rotation: geodesy and geoscience III posters. *Eos Trans AGU* 88(52), Fall Meet. Suppl., Abstract No: G43C-1480
- Kalarus M, Kosek W, Schuh H (2008) Summary of the Earth orientation parameters prediction comparison campaign. EGU General Assembly 2008, EGU abstract: EGU2008-A-00595
- Kalarus M, Luzum BJ, Lambert S, Kosek W (2006) Modelling and prediction of the FCN. In: *Proceedings of the journées 2005 systèmes de référence spatio-temporels*, pp 181–184
- Kosek W, Kalarus M, Niedzielski T (2008) Forecasting of the Earth orientation parameters—comparison of different algorithms. In: Capitaine N (ed) *Proceedings of the journées 2007, systèmes de référence spatio-temporels “The celestial reference frame for the future”*. Observatoire de Paris Systemes de Référence Temps-Espace UMR8630/CNRS, Paris, France, pp 155–158
- Kosek W, Rzeszótka A, Popiński W (2006) Phase variations of oscillations in the Earth orientation parameters detected by the wavelet technique. In: *Proceedings of the journées 2005 systèmes de référence spatio-temporels*, pp 121–124
- Kosek W (2010a) Future improvements in EOP prediction. In: *Proceedings of the IAG 2009, “Geodesy for planet earth”, August 31–September 4, 2009, Buenos Aires, Argentina* (accepted)
- Kosek W (2010b) Causes of prediction errors of pole coordinates data. In: *Proceedings of the 6th Orlov’s conference, “The study of the Earth as a planet by methods of geophysics, geodesy and astronomy”*, June 22–24, 2009. MAO NAS of Ukraine, Kiev, Ukraine, pp 96–103
- Luzum BJ, Wooden W, McCarthy DD, Schuh H, Kosek W, Kalarus M (2007) Ensemble prediction for Earth orientation parameters. EGU General Assembly 2007, EGU abstract: EGU2007-A-04315
- McCarthy DD (1996) IERS Conventions. IERS Technical Note 21, Observatoire de Paris
- McCarthy DD, Luzum BJ (1991) Prediction of Earth orientation. *Bull Geod* 65:18–22
- McCarthy DD, Petit G (2004) IERS conventions (2003). International Earth Rotation and Reference Systems Service (IERS)
- Tabachnick BD, Fidell LS (1996) *Using multivariate statistics*, 3rd edn. Harper Collins, New York